International Journal of Cell and Biomedical Science (2026) 5: (14) 591-607
https://doi.org/10.59278/cbs.v5i14.116

ORIGINAL ARTICLE OPEN ACCESS

An *in silico* Study of Carotenoids as Antioxidants through the KEAP1-NRF2 Pathway

Assyafiya Salwa,[1]* Niken Rahmah Ghanny,[2] Komang Ardi Wahyuningsih[3]

*Correspondence:
assyafiya.salwa@upnvj.ac.id

[1]*Department of Histology, Faculty of Medicine, Universitas Pembangunan Nasional Veteran Jakarta, Jakarta, Indonesia, 12450 ORCID ID: 0009-0006-4058-4137*
[2]*Department of Biochemistry, Faculty of Medicine, Universitas Pembangunan Nasional Veteran Jakarta, Jakarta, Indonesia, 12450 ORCID ID: 0009-0005-4909-4786*
[3]*Department of Histology,School of Medicine and Health Sciences, Atma Jaya Catholic University of Indonesia, Jakarta, Indonesia, 12450 ORCID ID: 0000-0002-5549-6571*

Submission August 29, 2026
Accepted October 09, 2026
Available online on October 31, 2026

©2026 The Authors. Published by Stem Cell and Cancer Research, Semarang, Indonesia. This is an open-access article under the terms of the Creative Commons Attribution-NonCommercial-ShareAlike License (CC BY-NC-SA 4.0), which permits unrestricted use, distribution, and reproduction in any medium, provided the original author and source are credited.

ABSTRACT

Background: Oxidative stress contributes to the pathogenesis of numerous degenerative diseases, and activation of the Kelch-like ECH-associated protein 1 (KEAP1)–nuclear factor erythroid 2-related factor 2 (NRF2) pathway represents a potential antioxidant strategy. **Aim:** This study evaluated the potential of eight carotenoids to inhibit the KEAP1–NRF2 protein–protein interaction through binding to the KEAP1 Kelch domain. **Methods:** Molecular docking was performed using the human KEAP1 crystal structure (PDB ID: 4L7D) and the co-crystallized ligand 1VX as a reference. The tested carotenoids were α-carotene, β-carotene, β-cryptoxanthin, lycopene, lutein, zeaxanthin, astaxanthin, and fucoxanthin. The top-ranked compound was subsequently evaluated by a 50-ns molecular dynamics simulation and in silico pharmacokinetic and toxicity prediction. **Results:** Among the tested compounds, β-carotene showed the most favorable docking affinity (−9.95 kcal/mol; predicted Ki: 51.10 nM), which was close to that of 1VX (−10.20 kcal/mol; predicted Ki: 33.47 nM). β-Carotene occupied the KEAP1 Kelch binding pocket through extensive hydrophobic interactions involving Tyr334, Tyr572, Phe577, Ala556, Arg415, and Arg336. Molecular dynamics simulation supported complex stability, with mean RMSD, RMSF, and radius of gyration values of 1.58 Å, 0.90 Å, and 17.91 Å, respectively. The KEAP1–β-carotene complex showed an average binding free energy of −22.57 kJ/mol, with persistent interactions at Tyr334 and Arg415. ADMET prediction indicated low oral bioavailability (0.17) and noncompliance with Lipinski's Rule of Five, although β-carotene complied with Veber's rule and was predicted to be non-hepatotoxic. **Conclusion:** In conclusion, β-carotene is a promising carotenoid scaffold for targeting the KEAP1 Kelch domain and potentially modulating NRF2 signaling.

Keywords: β-carotene; KEAP1–NRF2 pathway; molecular docking; molecular dynamics; oxidative stress; ADMET.

INTRODUCTION

Degenerative diseases such as cardiovascular disease, diabetes mellitus, and cancer are strongly influenced by oxidative stress as a key pathogenic mechanism. Oxidative stress arises from an imbalance between free radical production and endogenous antioxidant capacity, leading to cellular damage, mitochondrial dysfunction, increased apoptosis, and chronic inflammation.[1] Nuclear factor erythroid 2-related factor 2 (NRF2), encoded by the Nfe2l2 gene, is a transcription factor that plays a central role in maintaining redox homeostasis through the activation of endogenous antioxidant genes. Under physiological conditions, NRF2 is bound to Kelch-like ECH-associated protein (KEAP1) in the cytoplasm and is continuously degraded via ubiquitination. Upon activation, NRF2 translocates to the nucleus, heterodimerizes with small Maf proteins, and binds to the antioxidant response element (ARE),

thereby upregulating cytoprotective enzymes such as NAD(P)H quinone dehydrogenase 1 (NQO1) and components of the glutathione system.[1–4] Activation of the NRF2-ARE pathway has been shown to confer protective effects against oxidative stress, inflammation, and electrophilic stress across multiple degenerative conditions, including cardiovascular disease, cancer, and diabetes.[5]

There are two categories of molecules according to how they interfere with the binding between NRF2 and KEAP1: cysteine-binding activators and KEAP1-NRF2 protein-protein interaction (PPI) inhibitors. The molecule binds to cysteine on KEAP1 (Cys273, Cys288, and Cys297). However, the ability of molecules to interact with cysteine residues can cause off-target binding and context-dependent toxicity. The inhibitor system of KEAP1-NRF2 PPI can be an alternative strategy by disturbing the NRF2 interaction with the Kelch domain in KEAP1, specifically, form hydrophobic interactions with Tyr334, Tyr525, Tyr572, and Tyr577 and hydrogen bonds or salt bridges with Ser363, Arg380, Asn382, Arg415, Arg483, Ser508, and Ser555.[6]

Natural bioactive compounds have gained increasing attention as potential modulators of the KEAP1-NRF2 pathway because of their structural diversity and generally favorable biological safety profiles[1,4,7]. Carotenoids are a group of lipophilic pigments widely distributed in fruits, vegetables, algae, and microorganisms. In addition to their established role as free radical scavengers and singlet-oxygen quenchers, several carotenoids have been reported to modulate cellular signaling pathways associated with oxidative stress and inflammation. However, the ability of carotenoids to interact directly with the KEAP1 Kelch domain has not been sufficiently characterized.[8]

Molecular docking and molecular dynamics simulations provide useful approaches for evaluating ligand binding models, identifying interacting amino acid residues, and estimating the stability of protein-ligand complexes. Therefore, this study investigated the potential interaction of eight carotenoids with the KEAP1 Kelch domain using molecular docking. The most promising candidate was further analyzed through molecular dynamics simulations, pharmacokinetic prediction, and toxicity prediction. This study was designed to identify a carotenoid scaffold with potential activity against the KEAP1-NRF2 protein interaction and to provide a basis for subsequent experimental validation.

MATERIALS AND METHODS

Ligand and Protein Preparation

The crystal structure of the human KEAP1 Kelch domain co-crystallized with 1VX (PDB ID: 4L7D; resolution: 2.25 Å) was retrieved from the RCSB Protein Data Bank. The co-crystallized ligand 1VX was selected as a positive reference because its experimentally determined binding pose and reported inhibitory IC50 of 750 nM provide structural and activity references for the present computational study. 1VX, the co-crystallized ligand, is an NRF2 activator and a direct inhibitor of the NRF2-KEAP1 complex. This ligand has an IC50 value of 0.75 ± 0.32 µmol. Water and heteroatoms or ligands were removed, polar hydrogens were added, and Kollman charges were assigned to the target protein.

The three-dimensional structures of eight carotenoid candidates α-carotene (CID: 6419725), β-carotene (CID: 5289489), β-cryptoxanthin (CID: 5281235), lycopene (CID: 446925), lutein (CID: 5281243), zeaxanthin (CID: 5280899), astaxanthin (CID: 5281224), and fucoxanthin (CID: 5281239) were retrieved in SDF format from the PubChem database (https://pubchem.ncbi.nlm.nih.gov/). These carotenoids were selected as ligand candidates based on their reported antioxidant activity and potential to modulate the KEAP1-NRF2 signaling

pathway. Ligand structures were energy-minimized and converted to PDBQT using PyRx 0.8 version 32 bit, with all rotatable bonds set to allow torsional flexibility during docking. [9]

Molecular Docking

Molecular docking was performed using AutoDockTools version 1.5.7. A grid box was defined to cover the binding pocket of KEAP1, with dimensions of (X x Y x Z) centered at coordinates (X = -25.311, Y = 17.946, Z = -17.497). Polar hydrogen atoms were added to the Keap1 protein structure, and each docking experiment consisted of 50 runs. Docking results were ranked based on the predicted binding affinity for each ligand-protein complex. The carotenoid exhibiting the lowest or most negative binding energy, indicating the strongest predicted binding affinity to the protein KEAP1, was selected as the highest potential to disrupt the KEAP1-NRF2 interaction. Protein-ligand interactions of the top candidate, including hydrogen bonds and hydrophobic contacts with key binding residues, were visualized and analyzed using Discovery Studio Visualizer.

Molecular dynamics simulation

Molecular dynamics (MD) simulations were performed using software YASARA Structure version 26.8.9 (YASARA Biosciences GmbH, Vienna, Austria). A protein–ligand complex consisting of KEAP1 and the most promising ligand served as the initial structure for the simulation. Before the simulation, the entire complex was inspected to verify structural integrity, including the presence of amino acid residues. System preparation involved processing the protein structure through cleaning, hydrogen bond network optimization, and determination of protonation states at pH 7.4.[10] The system was then placed in a simulation cell with periodic boundary conditions, solvated with water molecules, and automatically supplemented with Na+ and Cl- ions to achieve physiological concentrations.[11,12] Before the production simulation, the system underwent energy minimization to alleviate geometric strain in the initial structure [11,13]. Simulations were conducted using the AMBER14 force field provided within the YASARA system. Long-range electrostatic interactions were calculated using Particle Mesh Ewald (PME), while short-range non-bonded interactions were computed using an 8 Å cut-off.[14–16]

Production simulations were run for 50 ns (50,000 ps) at 298 K using the YASARA macro `md_run.mcr`. Subsequently, the simulation data were analyzed using YASARA analysis modules to evaluate root mean square deviation (RMSD), root mean square fluctuation (RMSF), radius of gyration (Rg), binding energy (MM/PBSA), principal component analysis (PCA), and pair interaction occupancy. All data were exported in `.tab` format and visualized as graphs to facilitate result interpretation.

Pharmacokinetic and toxicity prediction

Following the molecular docking and molecular dynamics simulation, the selected carotenoid candidates were further evaluated for their pharmacokinetic properties and potential toxicity profiles. The ADMET prediction analysis was performed to assess the drug-likeness characteristics, absorption, distribution, metabolism, excretion, and toxicity parameters of the evaluated compounds. The predicted pharmacokinetic properties, including molecular weight, lipophilicity (logP), hydrogen bond donors (HBD), hydrogen bond acceptors (HBA), gastrointestinal absorption, and toxicity parameters. The physicochemical and pharmacokinetic properties of the selected carotenoid candidates were predicted using the SwissADME web server (https://www.swissadme.ch/). Toxicological profiles, including predicted oral rat acute toxicity (LD50) and other relevant endpoints, were evaluated using the pkCSM pharmacokinetics platform (https://biosig.lab.uq.edu.au/pkcsm/. These predictions were used to characterize the

pharmacokinetic properties and potential toxicity of the carotenoid candidates and to complement the docking-based assessment.

RESULTS

Molecular docking simulations were performed to evaluate the binding affinity of eight carotenoid candidates to the KEAP1 domain (PDB ID: 4L7D), using the co-crystallized ligand 1VX as a reference. The predicted binding energies, inhibition constant (Ki), and interactive residues of all candidates are summarized in Table 1. Among the eight carotenoids tested, β-carotene exhibited the strongest binding affinity, with a binding energy of -9.95 Kcal/mol and an estimated Ki value of 51.10 nM, followed by α-carotene (-9.61 Kcal/mol; 89.84 nM) and β-cryptoxanthin (-9.15 Kcal/mol; 197.16 nM). These three candidates showed binding energies closest to the native ligand 1VX (-10.20 Kcal/mol), suggesting a comparable capacity to occupy the kelch domain binding pocket of KEAP1. In contrast, lycopene, fucoxanthin, and lutein showed moderate binding affinities (-8.76, -8.22, and -8.30 Kcal/mol), respectively. Meanwhile, zeaxanthin and astaxanthin showed the weakest predicted interactions among the tested candidates, with binding energies of -7.60 kcal/mol and -6.86 kcal/mol.

According to Table 1, the interaction profile of the native ligand demonstrated a combination of hydrogen bonding and hydrophobic stabilization within the KEAP1 binding pocket. Ligand 1VX formed hydrogen bonds with Arg415, Arg483, and Ser508, along with hydrophobic interactions involving Tyr525, Ala556, and Tyr572. In contrast, β-carotene did not establish conventional hydrogen bond due to the absence of polar functional groups. Instead, β-carotene exhibited extensive hydrophobic interactions with several residues within the binding pocket, including Tyr334, Arg336, Ser363, Arg415, Tyr572, and Phe577. Similarly, α-carotene and β-cryptoxanthin (Figure 3 and Figure 4) displayed a similar interaction profile to β-carotene, particularly through hydrophobic interactions with Tyr334, Arg336, Ser363, Arg415, Tyr572, and Phe577. Lycopene (Figure 5) also interacted with several key residues, such as Tyr334, Arg336, Arg415, Tyr525, Ala556, Tyr572, and Phe577.

The oxygenated carotenoids, or xanthophyll-carotenoid group, showed additional polar interactions due to the presence of oxygen-containing functional groups. Fucoxanthin (Figure 6) interacted with Gln530 and Tyr572, while lutein and zeaxanthin (Figures 7 and Figure 8) interacted with Val463, and astaxanthin (Figure 9) formed hydrogen bonds with Val463 and Gly417. Nevertheless, these polar interactions did not contribute to the binding energy relative to β-carotene, α-carotene, and β-cryptoxanthin. Based on the lowest binding energy, β-carotene was selected as the candidate with the highest predicted binding affinity toward the KEAP1-Kelch domain among the eight carotenoids evaluated and was therefore prioritized for subsequent pharmacokinetic/toxicity prediction and in vitro validation.

The binding poses of the native ligand 1VX and selected carotenoid candidates within the KEAP1-Kelch domain were further analyzed through two-dimensional and three-dimensional interaction visualization. The native ligand 1VX occupied the central region of the KEAP1 binding pocket and exhibited a combination of hydrogen bonding and hydrophobic interactions that contributed to complex stabilization. Hydrogen bond interactions with Arg415, Arg483, and Ser508, together with hydrophobic contacts involving Tyr525, Tyr527, and Ala556, supported the stable accommodation of 1VX within the Kelch domain (Figure 1).

β-carotene showed a similar binding orientation as the native ligand in the same binding pocket, but did not form conventional hydrogen-bond interactions. The docking pose demonstrated (Figure 2) that β-carotene was mostly stabilized by large hydrophobic and van der Waals interactions with important residues like Tyr334, Ser363, Arg415, Ala556, Tyr572, and Phe577.

1VX occupies the same binding region, suggesting that β-carotene might interact with residues involved in the KEAP1 recognition pocket.

α-carotene and β-cryptoxanthin assumed similar orientations within the binding cavity, with their interactions occurring mostly via hydrophobic contacts. The oxygenated carotenoids, such as fucoxanthin, lutein, zeaxanthin, and astaxanthin, showed additional polar interactions through H-bonding as compared to the non-oxygenated carotenoid. However, the overall binding stability was lower than that of β-carotene. The visualization results agreed with the docking score, and β-carotene showed the most favorable interaction pattern among the evaluated carotenoid candidates.

According to the molecular docking results (Table 1), β-carotene had the highest binding energy and was closest to the native ligand compared to other carotenoids. KEAP1-β-carotene was selected for molecular dynamics simulation. The molecular dynamics simulation results indicated that the KEAP1-β-carotene complex maintained a highly stable and compact structural profile throughout the simulation. This was reflected by low average RMSD (Figure 10) and RMSF (Figure 11) values of 1.58 Å and 0.90 Å, respectively, together with a consistent radius of gyration (Rg) (Figure 12) of 17.91 Å. The complex also exhibited favorable binding energetics, with an average binding free energy of −22.57 kJ/mol (Figure 13). Notably, the system reached its global minimum energy state at 29 ns, achieving an optimal energy value of −36.048 kJ/mol. Key interactions were preserved with 100% occupancy, involving hydrophobic, π–π, and cation–π interactions at Tyr334 and Arg415. Collectively, these findings suggest that the ligand formed a persistent and energetically favorable complex with the target protein.

The drug-likeness and toxicity prediction results for the eight carotenoids are presented in Table 2. None of the evaluated compounds fulfilled Lipinski's Rule of Five (Ro5), indicating potential limitations in oral drug-like properties, particularly due to their relatively large molecular size and high lipophilicity. Nevertheless, α-carotene, β-carotene, β-cryptoxanthin, lutein, zeaxanthin, and astaxanthin complied with Veber's rule, whereas lycopene and fucoxanthin did not. This suggests that most of the evaluated carotenoids may possess acceptable molecular flexibility and polar surface characteristics, although their overall oral drug-likeness remains limited. All compounds showed an identical predicted bioavailability score of 0.17, indicating generally low oral bioavailability. This finding is consistent with the hydrophobic nature of carotenoids which contributes to their poor aqueous solubility and can limit their gastrointestinal bioaccessibility and subsequent absorption. Lipid-based delivery systems, including nanoemulsions and liposomes, as well as other encapsulation strategies, may improve carotenoid solubilization, stability, and bioaccessibility, with the potential to enhance oral bioavailability[17–19]. Structural modification of β-carotene can be another alternative to improve this limitation, such as using amorphous solid dispersion hot-melt technology to improve water solubility.[20]

The predicted acute oral toxicity values varied among the compounds. Astaxanthin showed the highest predicted oral rat LD50 value (3.562 mol/kg), followed by zeaxanthin (3.545 mol/kg) and lutein (3.491 mol/kg), suggesting relatively lower acute toxicity compared with the other carotenoids. In contrast, α-carotene displayed the lowest LD50 value (2.065 mol/kg), followed by β-carotene (2.134 mol/kg). However, all tested compounds were predicted to be non-hepatotoxic. Overall, these results indicate that the evaluated carotenoids have a favorable preliminary hepatic safety profile, although their low predicted oral bioavailability and failure to meet Ro5 criteria should be considered in further development.

International Journal of Cell and Biomedical Science (2026) 5: (14) 591-eee
https://doi.org/10.59278/cbs.v5i14.116

Table 1. Binding affinity calculation of α-carotene, β-carotene, β-cryptoxanthin, lycopene, lutein, zeaxanthin, astaxanthin, and fucoxanthin.

Ligand	Binding energy (Kcal/mol)	Ki	Interactive Residues
Native ligand (1VX)	-10.20	33.47 nM	Hydrogen bonds: Arg415, Arg483, Ser508 Hydrophobic interaction: Tyr525 (Pi-sigma), Tyr572 (Pi–pi T-shaped), Ala556 (Alkyl / pi–alkyl) van der Waals: Ser363, Gly364, Gly462, Gly509, Gln530, Ser555, Ser602, Gly603, Phe478, Tyr334, Phe577
β-carotene	-9.95	51.10 nM	Hydrophobic interaction: Arg336, Tyr334, Phe577, Ala556, Ser363, Arg415 (Alkyl / pi–alkyl) dan Tyr572 (Pi-sigma) van der Waals: Ser363, Gly364, Leu365, Ala366, Ile416, Gly417, Gly462, Val463, Gly464, Gly509, Ala510, Gly511, Leu557, Ser602, Gly603
α-carotene	-9.61	89.84 nM	Hydrophobic interaction: Tyr572, Tyr334, Phe577 (Pi-alkyl), Ala556, Ala366, Arg415, Arg336 (Alkyl / pi-alkyl) van der Waals: Gly511, Leu557, Gly603, Gly509, Ala510, Gly464, Val463, Gly462, Gly364, Ser363, Gly417, Ile416, Leu365
β-cryptoxanthin	-9.15	197.16 nM	Hydrophobic interaction: Tyr334, Tyr572, Phe577 (Pi-alkyl), Ala556, Ala366, Arg415, Arg336 (Alkyl / pi-alkyl) van der Waals: Leu557, Gly511, Gly509, Ala510, Val512, Gly462, Ser363, Ser602, Gly603, Val463, Gly464, Gly417, Val465, Ile416, Leu365, Gly364
Lycopene	-8.76	380.51 nM	Hydrophobic interaction: Tyr334, Tyr525, Tyr572, Phe577 (Pi-alkyl), Arg336, Ala556, Arg415 (Alkyl / pi-alkyl) van der Waals: Phe335, Ser508, Gln530, Ser555, Ser602, Leu557, Gly558, Gly509, Ala510, Gly462, Gly364, Gly603, Val604, Gly605, Ala366, Leu365, Ile416, Val463, Gly417
Fucoxanthin	-8.22	944.07 nM	Hydrogen bond: Gln530, Tyr572 Hydrophobic interaction: Tyr334, Tyr525, Phe577 (Pi-alkyl), Ala556, Arg415 (Alkyl / pi-alkyl) van der Waals: Ser508, Gly509, Ser555, Gly603, Gly364, Ser363, Ser602, His575, Arg336
Lutein	-8.30	825.15 nM	Hydrogen bond: Val463 Hydrophobic interaction: Tyr572 (Pi–sigma), Tyr334, Phe577 (Pi-alkyl), Arg336, Ala556, Ala366, Arg415 (Alkyl / pi-alkyl) van der Waals: Leu557, Gly511, Gly509, Ala510, Ser602, Gly603, Gly364, Gly462, Ile416, Gly417, Leu365

International Journal of Cell and Biomedical Science (2026) 5: (14) 591-eee
https://doi.org/10.59278/cbs.v5i14.116

Zeaxanthin	-7.60	2.65 µM	Hydrogen bond: Val463 Hydrophobic interaction: Tyr572 (Pi–sigma), Tyr334, Phe577 (Pi-alkyl), Arg415, Ala556, Arg336 (Alkyl / pi-alkyl) van der Waals: Val418, Val465, Gly417, Ile416, Leu365, Gly462, Gly464, Ala510, Gly364, Gly509, Leu557, Gly511, Ser602, Gly603
Astaxanthin	-6.86	9.25 µM	Hydrogen bond: Val463, Gly417 Hydrophobic interaction: Tyr334, Tyr572, Phe577 (Pi-alkyl), Arg415, Ala556, Arg336 (Alkyl / pi-alkyl) van der Waals: Val418, Ala366, Val465, Ile416, Leu365, Gly462, Gly603, Gly364, Ser602, Ser363, Gly509, Leu557, Gly511, Val512, Ala510, Gly464

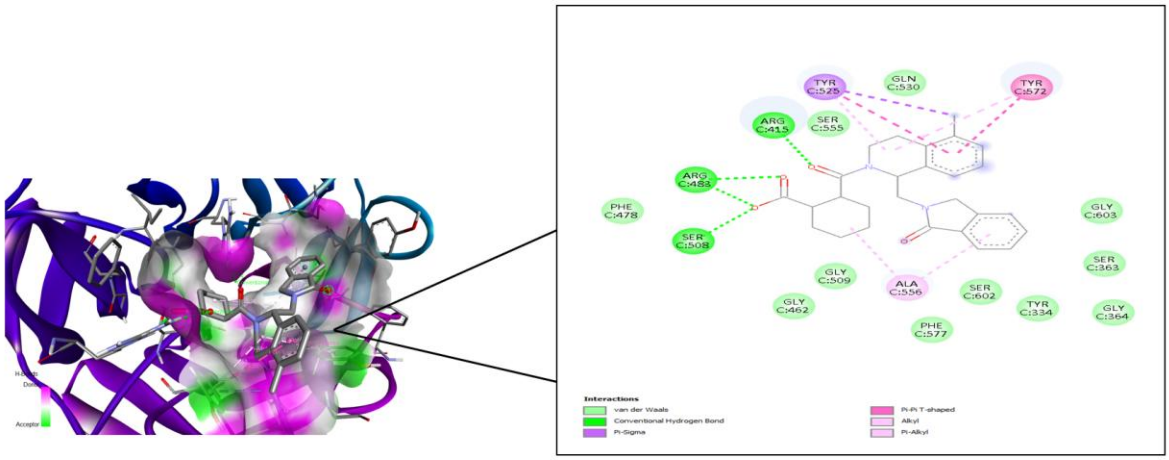


Figure 1. Conformation of 1VX (native ligand) and KEAP1 protein.

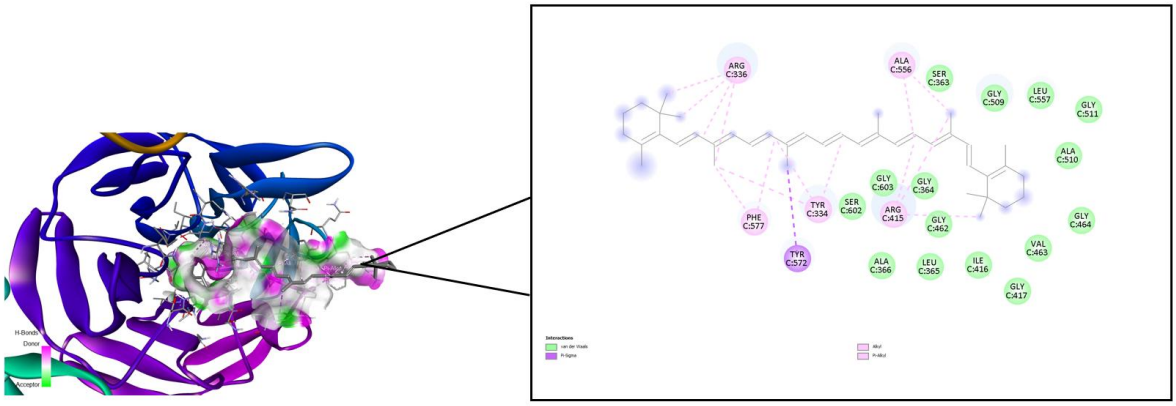


Figure 2. Conformation of β-carotene and KEAP1 protein.

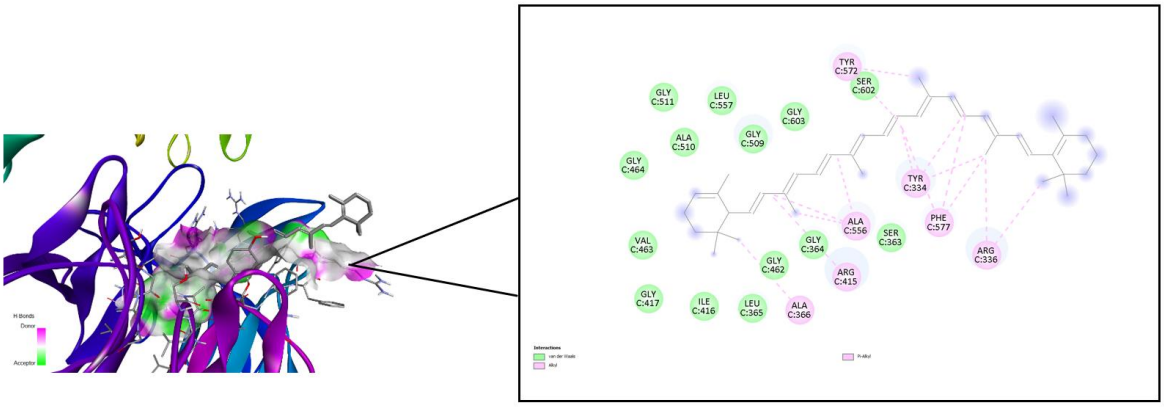


Figure 3. Conformation of α-carotene and KEAP1 protein

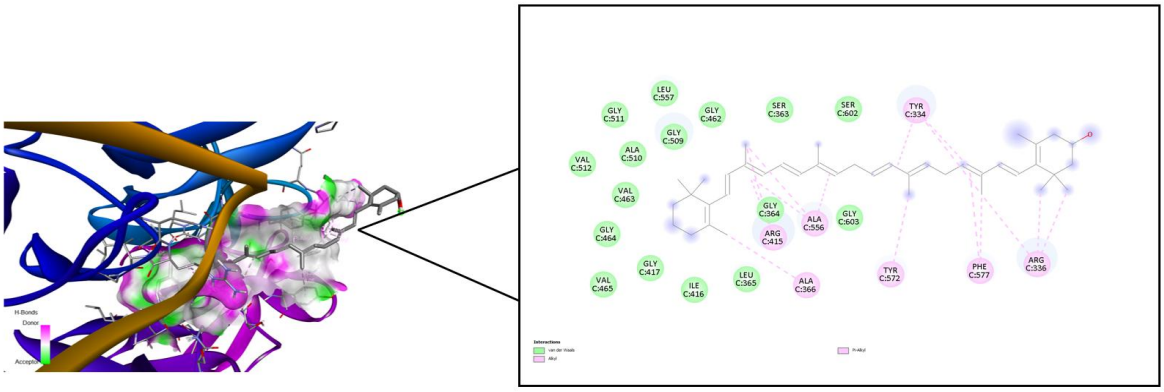


Figure 4. Conformation of β-cryptoxanthin and KEAP1 protein

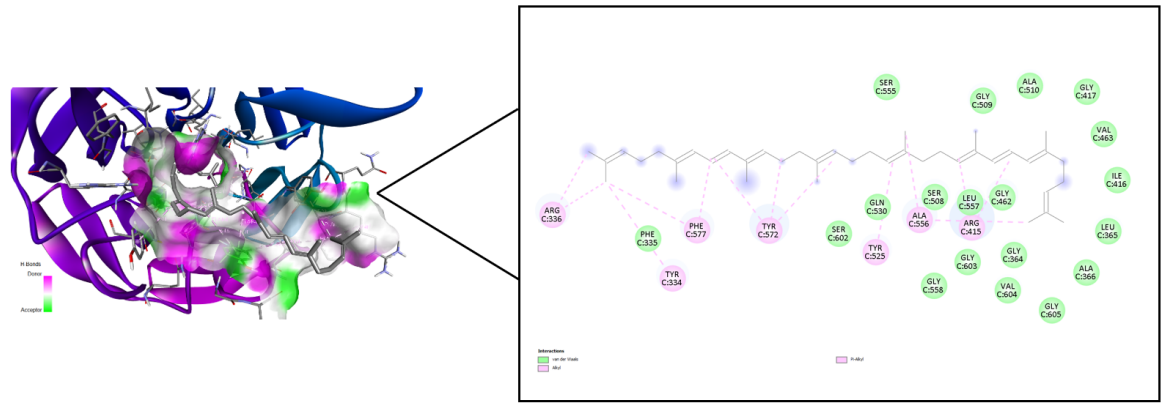


Figure 5. Conformation of lycopene and KEAP1 protein

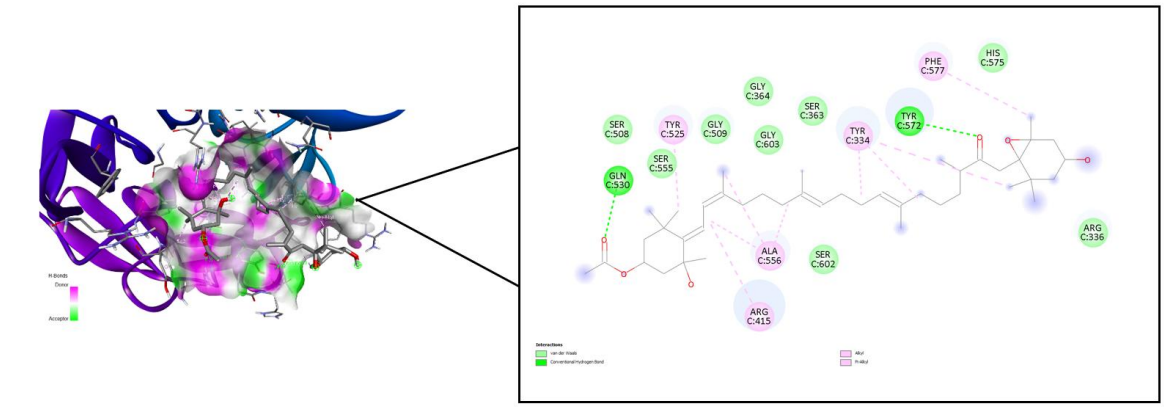


Figure 6. Conformation of fucoxanthin and KEAP1 protein

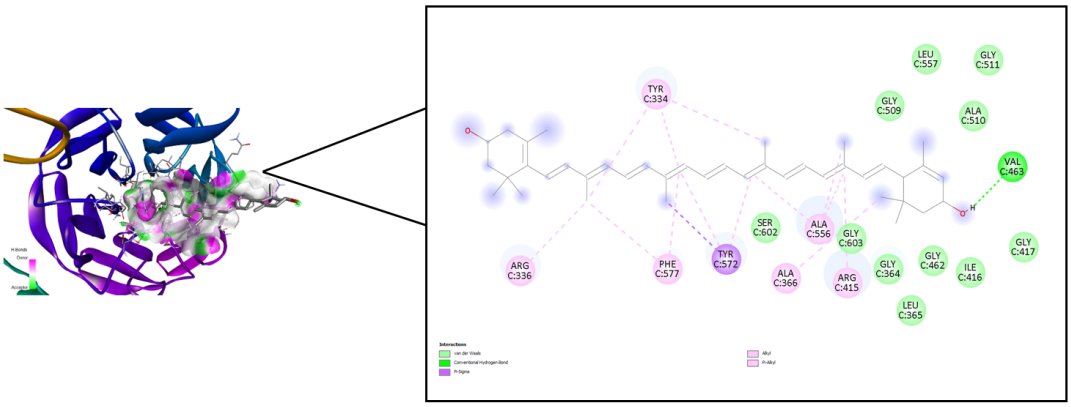


Figure 7. Conformation of lutein and KEAP1 protein

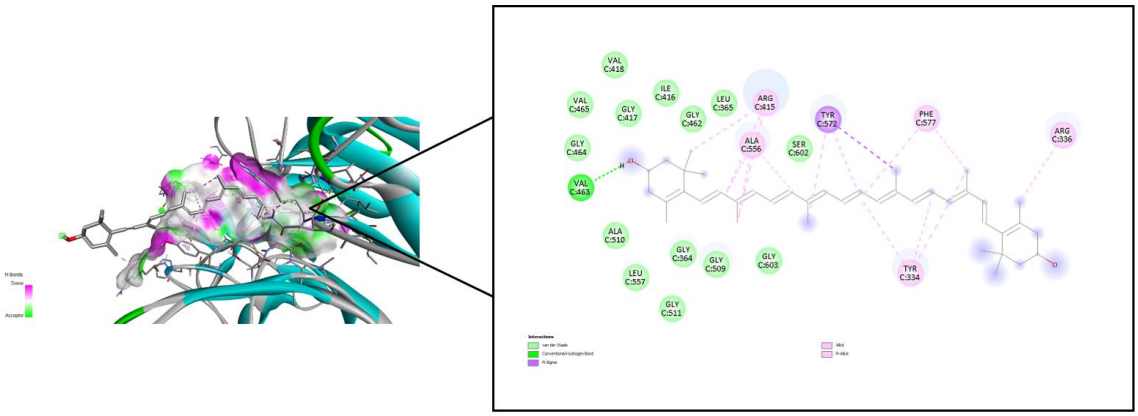


Figure 8. Conformation of zeaxanthin and KEAP1 protein

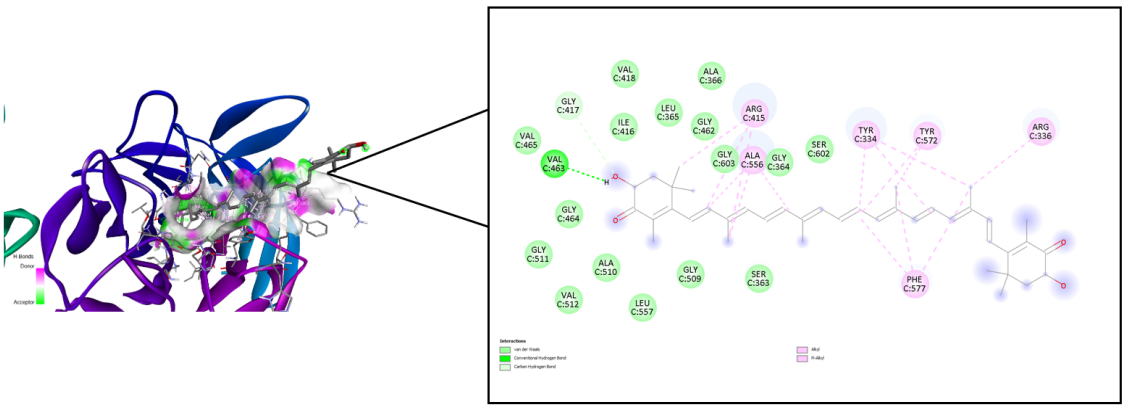


Figure 9. Conformation of astaxanthin and KEAP1 protein

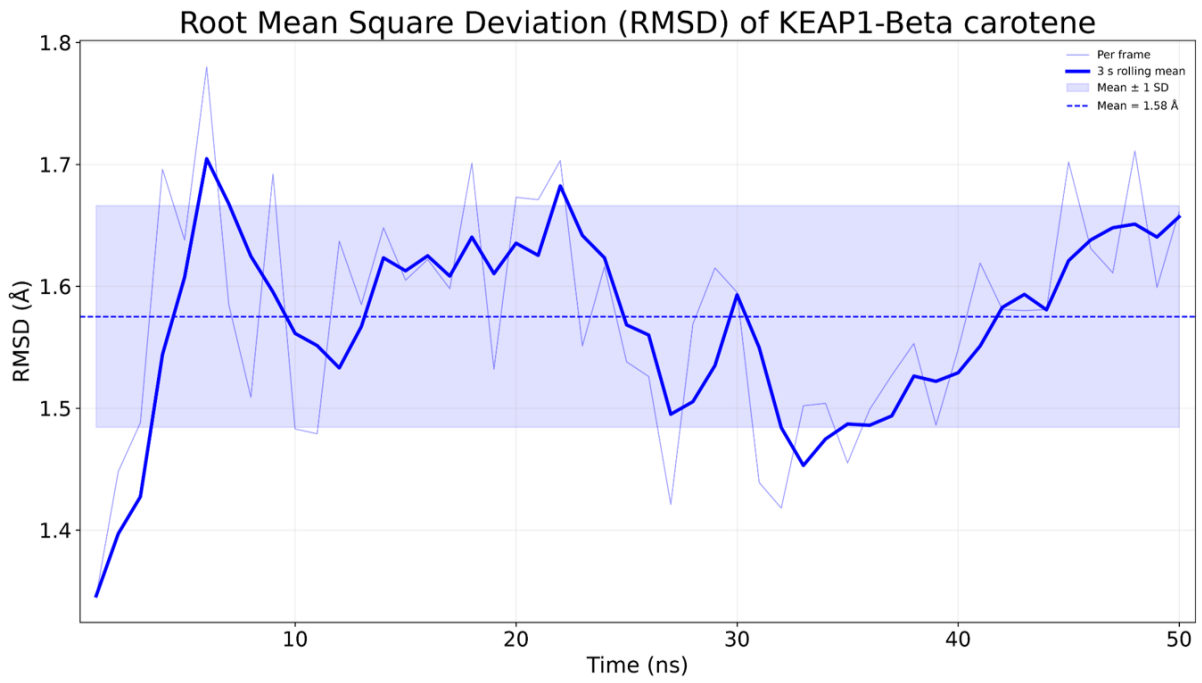


Figure 10. Structural stability analysis of KEAP1 based on the RMSD (Å) trajectory over simulation time (ns) with β-carotene

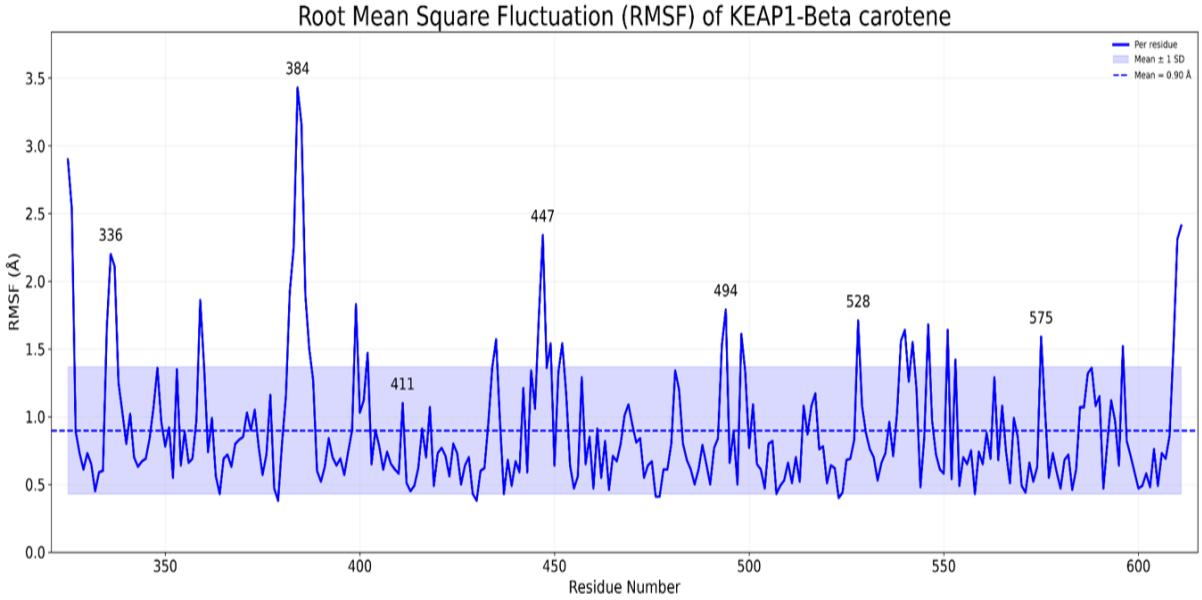


Figure 11. Fluctuation profile (RMSF) of KEAP1 amino acid residues. The numbers above the peaks indicate the specific residue numbers exhibiting high fluctuation during the interaction with β-carotene.

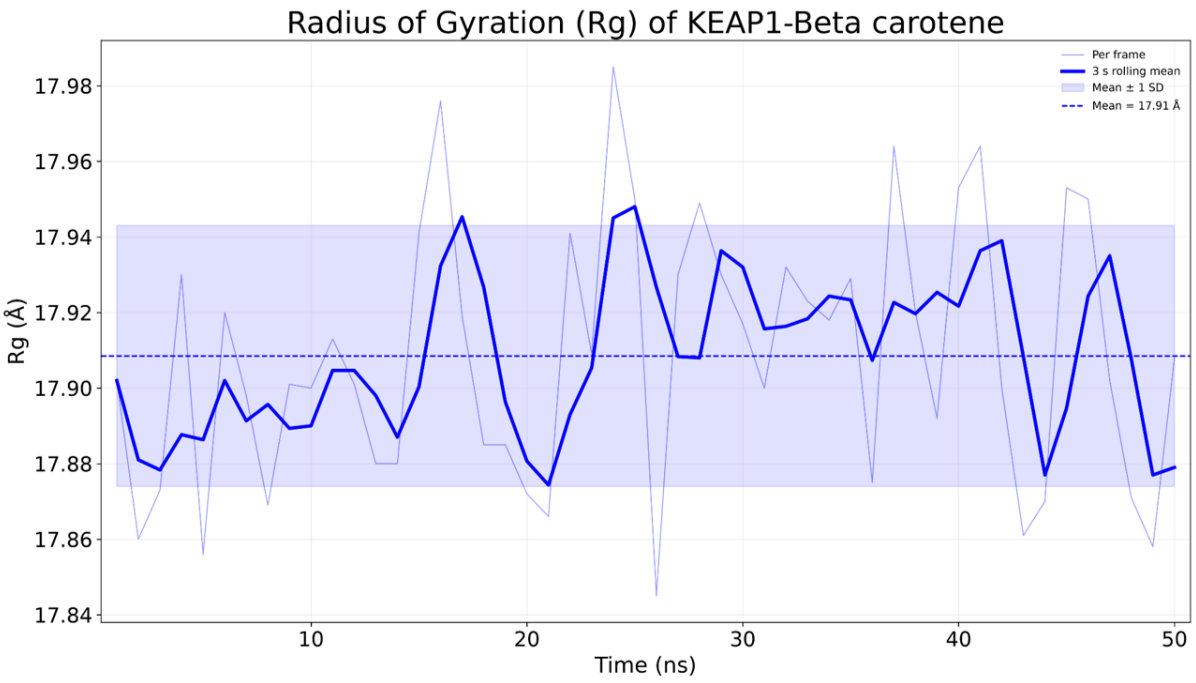


Figure 12. Analysis of KEAP1 structural compactness based on the Radius of Gyration (Rg) trajectory during a 50 ns MD simulation with β-carotene.

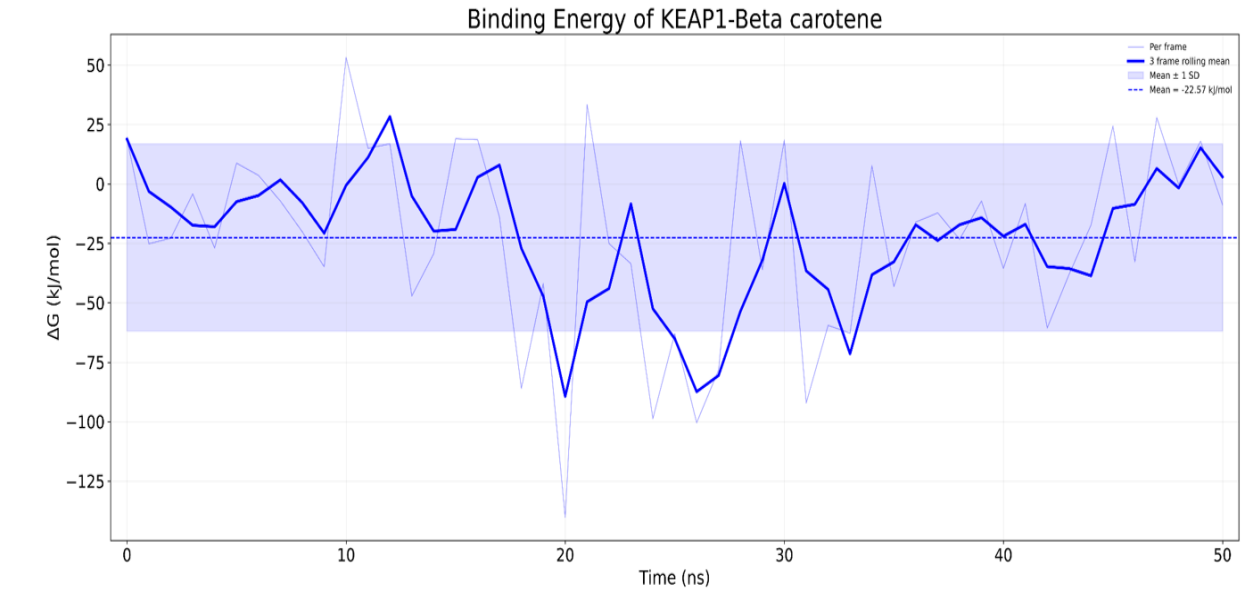


Figure 13. Binding energy profile (kJ/mol) of the KEAP1 interaction with β-carotene over simulation time (ns).

Table 2. Drug-likeness calculation of α-carotene, β-carotene, β-cryptoxanthin, lycopene, lutein, zeaxanthin, astaxanthin, and fucoxanthin.

Compounds	Molecular weight g/mol	Ro5	Veber rule	Bioavailability	Oral Rat Acute Toxicity (LD50) (mol/kg)	Hepatotoxicity
α-carotene	536.89	No	Yes	0.17	2.065	No
β-carotene	536.87	No	Yes	0.17	2.134	No
β-cryptoxanthin	552.87	No	Yes	0.17	2.233	No
Lycopene	536.9	No	No	0.17	2.224	No
Lutein	568.9	No	Yes	0.17	3.491	No
Zeaxanthin	568.9	No	Yes	0.17	3.545	No
Astaxanthin	596.8	No	Yes	0.17	3.562	No
Fucoxanthin	658.92	No	No	0.17	2.47	No

NRF2 is a key regulator of antioxidant response. Within the nucleus, it triggers the production of enzymes and pathways related to antioxidant. KEAP1, a cysteine-rich regulatory protein, leads to NRF2 ubiquitylation and proteasomal degradation [21]. The native ligand (1VX) binds strongly to the NRF2 peptide (containing the ETGE or DLG motifs) recognition pocket in KEAP1 (six subpockets P1-P6) through a combination of hydrogen bonds with polar residues and aromatic-hydrophobic interactions that stabilize the ligand. The interaction pattern of 1VX includes two key elements of effective KEAP1 inhibitors: a polar anionic anchor that interacts with Arg415, Arg483, and Ser508 (subpocket P1) and a hydrophobic-aromatic scaffold maintained by Tyr525, Tyr572, and Ala556 (subpockets P4-P5). The carboxylic acid group of the native ligand is crucial as it acts as a hydrogen bond acceptor for positively charged arginine residues. This pattern mimics the recognition of NRF2-ETGE or DLG motifs by the KEAP1-Kelch domain[22,23]. By occupying the Kelch pocket, 1VX can interfere with the interaction between KEAP1 and NRF2 and potentially reduce NRF2 degradation. The present in silico study identified β-carotene as the most promising carotenoid candidate for interaction with the Kelch domain of Kelch-like ECH-associated protein 1 (KEAP1). Among the eight carotenoids evaluated, β-carotene showed the most favorable docking score. This affinity was close to that of the co-crystallized native ligand, indicating that β-carotene may effectively occupy the KEAP1 binding pocket.

Compared to the native ligand, hydrogen bonds were not observed in the interaction between KEAP1 and the carotenes, as they lack oxygen and nitrogen atoms. However, the xanthophyll group formed hydrogen bonds in the presence of oxygen[24]. The strongest interaction, KEAP1-β-carotene, suggested that the favorable docking of β-carotene was mainly driven by extensive nonpolar interactions. According to Figure 2, β-carotene interacted with similar subpocket P5 within the KEAP1 binding pocket, which are Tyr334, Phe577, and Tyr572 in hydrophobic interaction. This compound also interacted with other subpockets but in a different type of interaction, which is nonpolar binding (hydrophobic interactions) instead of polar binding (hydrogen bonds). The interactions involve several residues, which are Ala556 (subpocket P3), Ser363 (subpocket P2), and Arg415 (subpocket P1)[22,23]. KEAP1-β-carotene complex formed a new interaction outside the binding pocket of KEAP1-NRF2, which is at the Arg336 residue with a hydrophobic interaction. Although the native ligand formed

hydrogen bonds with Arg415, Arg483, and Ser508, β-carotene achieved a comparable binding score through hydrophobic and aromatic interactions. This finding is consistent with the highly lipophilic and extended polyene structure of β-carotene[24], which may enable broad surface complementarity and stable accommodation within the relatively hydrophobic regions of the KEAP1 pocket. This difference is mechanistically important: occupation of a similar region does not necessarily imply equivalent binding specificity or competitive activity. The extended nonpolar structure of β-carotene may enable favorable complementarity with portions of the pocket, but the absence of the polar anchoring interactions observed for 1VX leaves uncertainty regarding its ability to compete with NRF2. Moreover, the small difference between their docking scores should not be interpreted as evidence of comparable experimental potency. The reported inhibition constants are estimates derived from docking scores, not experimentally determined inhibitory concentrations. Thus, these results provide a rationale for testing direct binding and competition rather than establishing either property.

The molecular dynamics simulation further supported the stability of the KEAP1–β-carotene complex. The RMSD value was used to assess the average structural deviation from the initial conformation of the KEAP1–β-carotene complex. It is considered to be acceptable if the value is between 1-3Å. The low mean RMSD value indicated limited structural deviation (variability and stability) of the complex during the simulation[25–27], suggesting that β-carotene remained stable within the binding site. The flexibility of the protein was assessed using the RMSF value. It estimated the binding orientation of the ligand and the targeted protein's structural alteration of the residue at specific temperature and pressure. Strongly bound ligands with excellent protein stability and rigidity in the structures are indicated by protein RMSF values of ≤2.0 Å. The average RMSF of the KEAP1–β-carotene complex indicated generally low residue-level mobility, limited flexibility, and high protein stability, implying that ligand binding did not induce marked local destabilization of the protein structure[26,27]. The radius of gyration (Rg) was used to analyze the system compactness, and the value demonstrated that the complex remained compact throughout the simulation with consistent values, without evidence of substantial unfolding or expansion[26–28]. Together, RMSD, RMSF, and Rg parameters indicated that the binding of β-carotene was compatible with the conformational stability of KEAP1.

The binding-energy analysis also demonstrated favorable interactions between β-carotene and KEAP1, which attained a particularly favorable conformational state during the simulation. The contacts are relevant because they provide dynamic support for the docking prediction and suggest that the initially predicted pose was retained during the simulation period. The interaction between β-carotene and the KEAP1-Kelch domain is potentially relevant to modulation of the KEAP1–NRF2 signaling. The occupation of the Kelch domain by a ligand may interfere with substrate recognition and potentially reduce KEAP1-mediated repression of NRF2. This could promote NRF2 stabilization and enhance the transcription of antioxidant and cytoprotective genes.

The predicted drug-likeness profile introduces a further translational constraint (Table 2). β-carotene's unfavorable Lipinski classification indicates potential challenges for conventional oral small-molecule development, despite its compliance with Veber's rule. Importantly, the SwissADME bioavailability score of 0.17 is a rule-based probability score related to achieving at least 10% oral bioavailability in rats or measurable Caco-2 permeability; it does not mean that oral bioavailability has been measured or predicted to equal 17%. Therefore, this score should be interpreted as a screening indicator rather than a quantitative estimate of human systemic exposure.[29]

The predicted absence of hepatotoxicity should be treated as a preliminary screening result rather than confirmation of safety. The current toxicity predictions do not establish an effective exposure range, long-term tolerability, or safety under specific disease conditions. Future development should therefore combine experimental toxicity assessment with measurements of cellular and

systemic exposure. Overall, the contribution of this study is the prioritization of β-carotene and the formulation of a testable KEAP1-binding hypothesis. Confirmation of this hypothesis requires reproducible computational evidence, direct interaction measurements, demonstration of NRF2-dependent biological activity, and evaluation of delivery and safety limitations.

CONCLUSION

The *in silico* study evaluated eight carotenoids as potential modulators of the KEAP1–NRF2 protein–protein interaction. Among the evaluated compounds, β-carotene showed the most favorable predicted binding affinity toward the KEAP1 Kelch domain, approaching the affinity of the native ligand 1VX. Its interaction was predominantly mediated by hydrophobic contacts with key residues in and around the KEAP1–NRF2 recognition pocket. Molecular dynamics simulation further indicated that the KEAP1–β-carotene complex remained structurally stable and compact during 50 ns of simulation. These findings suggest that β-carotene may occupy the KEAP1 Kelch domain and has the potential to interfere with KEAP1-mediated NRF2 recognition.

Despite its favorable predicted binding profile and non-hepatotoxicity prediction, β-carotene demonstrated limited oral drug-likeness and low predicted bioavailability, likely related to its high lipophilicity and molecular size. Therefore, future studies should validate the KEAP1–β-carotene interaction experimentally through binding assays, cell-based NRF2 activation assays, and evaluation of downstream antioxidant gene expression. In addition, lipid-based or nanostructured delivery systems may be considered to improve its solubility, bioaccessibility, and systemic availability.

Acknowledgements

This research was fully funded by the **Hibah Eksternal DPPM Program BOPTN Program Penelitian Baru Tahun 2026 (255/C3/DT.05.00/PL-BARU/2026)** provided by the Indonesian Ministry of Higher Education, Research, and Technology.

Authors' contributions

Concepting - AS, NRG, KAW; Ligand and Protein Selection - AS; Molecular Docking - AS, NRG; ADMET - NRG; Data analysis - AS, NRG; Drafting manuscript: AS, NRG; Manuscript review and finalization: KAW

Conflict of interest

The authors declare that there are no conflicts of interest related to this work.

REFERENCES

1. Reddy VP. Oxidative Stress in Health and Disease. *Biomedicines*. 2023;11(11):2925. doi:10.3390/biomedicines11112925
2. Woo Y, Lee HJ, Jung YM, Jung YJ. mTOR-Mediated Antioxidant Activation in Solid Tumor Radioresistance. *J Oncol*. 2019;2019:1-11. doi:10.1155/2019/5956867
3. Tumilaar SG, Hardianto A, Dohi H, Kurnia D. A Comprehensive Review of Free Radicals, Oxidative Stress, and Antioxidants: Overview, Clinical Applications, Global Perspectives, Future Directions, and Mechanisms of Antioxidant Activity of Flavonoid Compounds. Ahmed M, ed. *J Chem*. 2024;2024:1-21. doi:10.1155/2024/5594386

4. Muscolo A, Mariateresa O, Giulio T, Mariateresa R. Oxidative Stress: The Role of Antioxidant Phytochemicals in the Prevention and Treatment of Diseases. *Int J Mol Sci*. 2024;25(6):3264. doi:10.3390/ijms25063264
5. Li R, Jia Z, Zhu H. Regulation of Nrf2 Signaling. *React Oxyg Species*. 2019;8(24):312-322.
6. De Vita S, González-Burgos E, Terracciano S, Chini MG, Gómez-Serranillos MP, Bifulco G. Discovery of New Antioxidant Molecules Enhancing the Nrf2-Mediated Pathway: Docking Studies and Biological Evaluation. *Int J Mol Sci*. 2026;27(4):1862. doi:10.3390/ijms27041862
7. De Vita S, González-Burgos E, Terracciano S, Chini MG, Gómez-Serranillos MP, Bifulco G. Discovery of New Antioxidant Molecules Enhancing the Nrf2-Mediated Pathway: Docking Studies and Biological Evaluation. *Int J Mol Sci*. 2026;27(4):1862. doi:10.3390/ijms27041862
8. Medina-García M, Baeza-Morales A, Martínez-Peinado P, et al. Carotenoids and Their Interaction with the Immune System. *Antioxidants*. 2025;14(9):1111. doi:10.3390/antiox14091111
9. Morris GM, Huey R, Lindstrom W, et al. AutoDock4 and AutoDockTools4: Automated docking with selective receptor flexibility. *J Comput Chem*. 2009;30(16):2785-2791. doi:10.1002/jcc.21256
10. Krieger E, Dunbrack RL, Hooft RWW, Krieger B. Assignment of Protonation States in Proteins and Ligands: Combining pKa Prediction with Hydrogen Bonding Network Optimization. In: Baron R, ed. *Computational Drug Discovery and Design*. Vol 819. Methods in Molecular Biology. Springer New York; 2012:405-421. doi:10.1007/978-1-61779-465-0_25
11. Harris JA, Liu R, De Oliveira VM, Montelongo EV, Henderson JA, Shen J. GPU-Accelerated All-atom Particle-Mesh Ewald Continuous Constant pH Molecular Dynamics in Amber. *Biophysics*. Preprint posted online June 5, 2022. doi:10.1101/2022.06.04.494833
12. Huggins D. Comparing the performance of different AMBER protein forcefields, partial charge assignments, and water models for absolute binding free energy calculations. Preprint posted online January 31, 2022. doi:10.26434/chemrxiv-2022-l69v9
13. Peeples CA, Liu R, Shen J. Force Field Limitations of All-Atom Continuous Constant pH Molecular Dynamics. *J Phys Chem B*. 2024;128(47):11616-11624. doi:10.1021/acs.jpcb.4c05971
14. Batcho PF, Case DA, Schlick T. Optimized particle-mesh Ewald/multiple-time step integration for molecular dynamics simulations. *J Chem Phys*. 2001;115(9):4003-4018. doi:10.1063/1.1389854
15. Krieger E, Darden T, Nabuurs SB, Finkelstein A, Vriend G. Making optimal use of empirical energy functions: Force-field parameterization in crystal space. *Proteins Struct Funct Bioinforma*. 2004;57(4):678-683. doi:10.1002/prot.20251
16. Krieger E, Vriend G. New ways to boost molecular dynamics simulations. *J Comput Chem*. 2015;36(13):996-1007. doi:10.1002/jcc.23899
17. Jalali-Jivan M, Rostamabadi H, Assadpour E, et al. Recent progresses in the delivery of β-carotene: From nano/microencapsulation to bioaccessibility. *Adv Colloid Interface Sci*. 2022;307:102750. doi:10.1016/j.cis.2022.102750
18. Molteni C, La Motta C, Valoppi F. Improving the Bioaccessibility and Bioavailability of Carotenoids by Means of Nanostructured Delivery Systems: A Comprehensive Review. *Antioxidants*. 2022;11(10):1931. doi:10.3390/antiox11101931
19. Patel J, Roy H, Khobragade DS, et al. Natural lipid-based nanoformulations for enhancing hepatoprotective activity: mechanisms, efficacy, and clinical translation. *Health Nanotechnol*. 2025;1(1):11. doi:10.1186/s44301-025-00010-8
20. Otani S, Miki S, Nakamura Y, Ishimoto K, Ago Y, Nakagawa S. Improved Bioavailability of β-Carotene by Amorphous Solid Dispersion Technology in Rats. *J Nutr Sci Vitaminol (Tokyo)*. 2020;66(2):207-210. doi:10.3177/jnsv.66.207

21. Culletta G, Buttari B, Arese M, et al. Natural products as non-covalent and covalent modulators of the KEAP1/NRF2 pathway exerting antioxidant effects. *Eur J Med Chem*. 2024;270:116355. doi:10.1016/j.ejmech.2024.116355
22. Crisman E, Duarte P, Dauden E, et al. KEAP1-NRF2 protein–protein interaction inhibitors: Design, pharmacological properties and therapeutic potential. *Med Res Rev*. 2023;43(1):237-287. doi:10.1002/med.21925
23. Jiang ZY, Lu MC, Xu L, et al. Discovery of Potent Keap1–Nrf2 Protein–Protein Interaction Inhibitor Based on Molecular Binding Determinants Analysis. *J Med Chem*. 2014;57(6):2736-2745. doi:10.1021/jm5000529
24. Borges CV, Orsi RO, Maraschin M, Lima GPP. Oxidative stress in plants and the biochemical response mechanisms. In: *Plant Stress Mitigators*. Elsevier; 2023:455-468. doi:10.1016/B978-0-323-89871-3.00022-7
25. Ding Y, Fang Y, Moreno J, Ramanujam J, Jarrell M, Brylinski M. Assessing the similarity of ligand binding conformations with the Contact Mode Score. *Comput Biol Chem*. 2016;64:403-413. doi:10.1016/j.compbiolchem.2016.08.007
26. Medoro A, Jafar TH, Sallustio F, Scapagnini G, Saso L, Davinelli S. Computational Assessment of Carotenoids as Keap1-Nrf2 Protein–Protein Interaction Inhibitors: Implications for Antioxidant Strategies. *Biochem Mosc*. 2024;89(10):1681-1691. doi:10.1134/S0006297924100031
27. Alzain AA, Mukhtar RM, Abdelmoniem N, et al. Modulation of NRF2/KEAP1-Mediated Oxidative Stress for Cancer Treatment by Natural Products Using Pharmacophore-Based Screening, Molecular Docking, and Molecular Dynamics Studies. *Molecules*. 2023;28(16):6003. doi:10.3390/molecules28166003
28. Singh E, Matada GSP, Dhiwar PS, Patil RB, Pal R. *In-silico* based discovery of potential Keap1 inhibitors using the strategies of pharmacophore screening, molecular docking, and MD simulation studies. *BioImpacts*. Published online September 14, 2024:1. doi:10.34172/bi.30335
29. Daina A, Michielin O, Zoete V. SwissADME: a free web tool to evaluate pharmacokinetics, drug-likeness and medicinal chemistry friendliness of small molecules. *Sci Rep*. 2017;7(1):42717. doi:10.1038/srep42717